Effects of pipe elbows and tube bundles on selected types of flowmeters

G. E. MATTINGLY and T. T. YEH

This paper presents experimental results for the decay of pipe elbow-produced swirl in pipeflows and its effects on flowmeter measurement accuracy. Experiments include the decay of swirl produced by single and double elbow configurations for pipe diameter Reynolds numbers of 10^4 to 10^5 using water in a 50 mm diameter facility at NIST in Gaithersburg, MD. Results show that different types of swirl are produced by the different piping configurations. The swirl decay is found to be dependent on the type of swirl and the pipe Reynolds number. At high Reynolds number very long lengths of straight, constant diameter pipe are required to dissipate the single eddy type swirl that is produced by the two elbows out-of-plane configuration. Without flow conditioning, it is concluded that the specifications of upstream pipe lengths in the current flowmetering standards may not be sufficient to achieve the desired flow metering accuracy.

Experimental results are also presented for the effects produced by tube bundle-type flow conditioners. These results show shifts in orifice meter discharge coefficients that are both positive and negative depending upon pertinent conditions. A range of orifice geometries, Reynolds numbers and meter locations are studied and explanations are put forth to explain these shifts. Results are also presented for a specific type of turbine meter. These show meter factor shifts that are also both positive or negative depending upon the type of swirl pattern entering this meter. An example is given in which the insertion of a tube bundle flow conditioner between a single elbow and the turbine meter produces a larger disturbance to the meter factor than would occur without the conditioner.

Keywords: swirl, measurement accuracy, pipe elbows, tube bundles

Introduction

The effects of swirl on orifice meter performance were initially observed in the US in the early 1900s[1, 2]. Consequently, early testing programmes, sponsored by the American Gas Association (AGA), were devised to describe and quantify these effects, see Appendix No. 3 in reference 1. These early US programmes were followed by others that were supported by the gas industry and other sources such as the American Society of Mechanical Engineers (ASME), the National Institute of Standards and Technology (NIST) and the American Petroleum Institute (API).

A better understanding of the effects of pipeflow swirl on practical flow measurements and related fluid mechanics phenomena can be obtained through experimental fluid metering research programmes that use the currently available flow research tools[2]. The results produced herein are considered to be the type of data that will be needed to improve current flow measurement standards and associated metering practice.

The authors are in the Fluid Flow Group, National Institute of Standards and Technology, Gaithersburg, Maryland, USA

The upstream pipe length requirements in two international orifice metering standards – ISO-5167 and ANSI/API-2530 – are quite different[1, 3]. ISO-5167 specifies that the upstream pipe length for a beta ratio = 0.75 (orifice hole to pipe diameter ratio) meter installed downstream of double elbows out-of-plane should be equal to or greater than 70 diameters (D); ANSI/API-2530 specifies $35D$ for the same conditions. The ISO standard also specifies that swirl angles should be less than $\pm 2°$ everywhere in the pipe cross-sectional area at the location where the meter is to be installed; the ANSI/API makes no such stipulation. In both of these standards, no dependence is given for the effects of the type of swirl, the Reynolds number, the pipe roughness etc.

This paper presents experimental data on: (1) the decay of two different types of swirl generated by conventional pipe elbow configurations, (2) the dependence of these swirls on Reynolds number and (3) the resulting swirl effects on the performance of specific types of flowmeters. The elbows used in this study have centreline curvature of $1.5D$. Results indicate that both of the standards mentioned above need to have the sections on installation specifications improved.

0955-5986/91/010004-10

The effects of flow conditioning devices, especially the tube bundle type, are included in orifice meter standards. Here, they are described as effective elements for reducing the lengths of upstream piping needed to reduce or eliminate shifts in discharge coefficient produced by swirl caused by piping effects. The experimental results presented here show that tube bundle type flow conditioners can have the opposite effect on both orifice and turbine meter performance.

Experimental procedure

Experiments in a NIST water flow facility have been used to characterize swirl decay in a 50 mm diameter pipe at Reynolds numbers of 10^4 and 10^5. Two different types of swirl were generated using two pipe arragements: (1) a single long radius elbow and (2) two long-radius elbows in an out-of-plane configuration. These configurations and the coordinate systems used are shown in Figure 1, where the flowrate is Q. Velocity profiles were measured with a laser Doppler velocimeter (LDV)[4]. These results have been produced in piping with surface roughness of 3 μm (relative roughness of 6×10^{-3}% based on D) as measured with a calibrated profilometer[5–8]. For each of these piping configurations, the entering pipeflow was that from the same, very long ($80D$) pipe which was preceded by several flow conditioners. When the flow from this unit of pipe work was measured using LDV, it was found that the mean velocity profile conformed to the power law distribution with the appropriate exponent[5–8].

Results

All of the pipeflow profile results shown below are for a diametral Reynolds number of 10^5.

Single elbow

Velocity profile measurements for the standard long-radius elbow are shown in Figure 2(a). These results pertain to different downstream distances from the elbow for a pipe Reynolds number of 10^5. Only two velocity components were measured: the streamwise component labelled W in the Z direction and the vertical component V in the Y direction, refer to Figure 1(a). Velocities and lengths are normalized using, respectively, the cross-sectional average of the axial velocity and the inner pipe diameter. The profiles for the ideal flows are denoted by the dashed lines. For an ideal flow, the vertical velocity is zero everywhere and the streamwise velocity profile is the pertinent power law distribution. The exponent for these conditions is taken to be 7. The centreline slope discontinuity associated with the power law distribution has been smoothed. The profile between $X = \pm 0.1$ is smoothed using a parabola based on the values at $X = \pm 0.1$ and ± 0.15. The data indicates that the standard long radius elbow produces a dual-eddy (defined here as type II) swirl pattern that has two counter-rotating vortices on either side of the centre plane of the elbow[7,8]. These vortices produce a strong transverse flow directed toward the outside of the elbow. The centre core of this flow is found to have axial velocities that are much slower than the corresponding ideal flow.

A time-averaged swirl angle can be defined as the arctangent of the mean vertical velocity component divided by the mean streamwise component, and results are shown in Figure 3(a). The results close to the elbow show that the transverse flow produced by the counter-rotating vortices give swirl angles of −14°

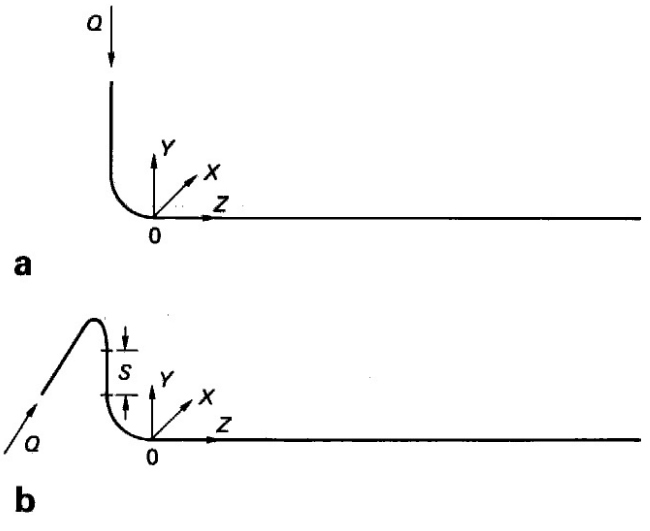

Figure 1 (a) Single elbow configuration; (b) double elbow out-of-plane configuration with spacing, s

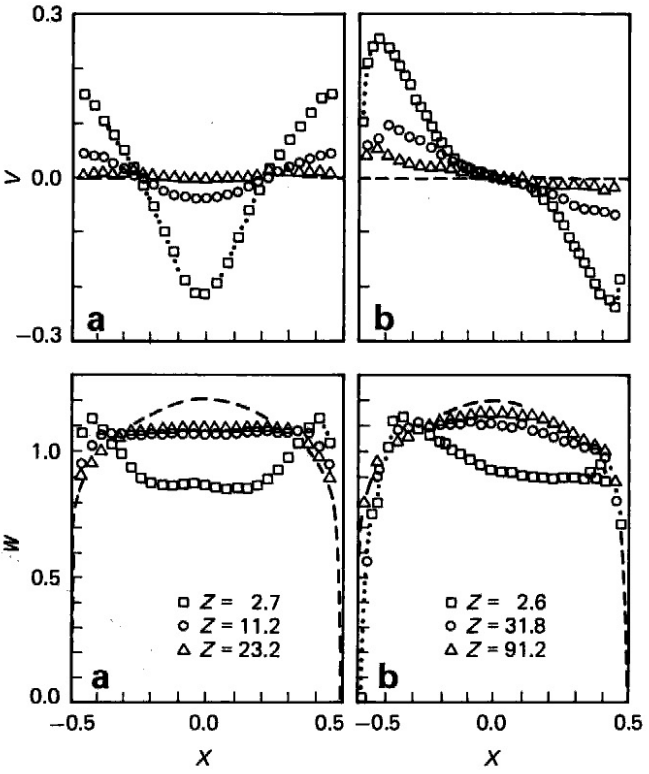

Figure 2 Vertical, V, and streamwise, W, velocity profiles along the horizontal diameter for: (a) the single elbow configuration, and (b) the closely coupled double elbows out-of-plane configuration. Downstream distances are in diameters. Ideal profiles are shown by dashed lines

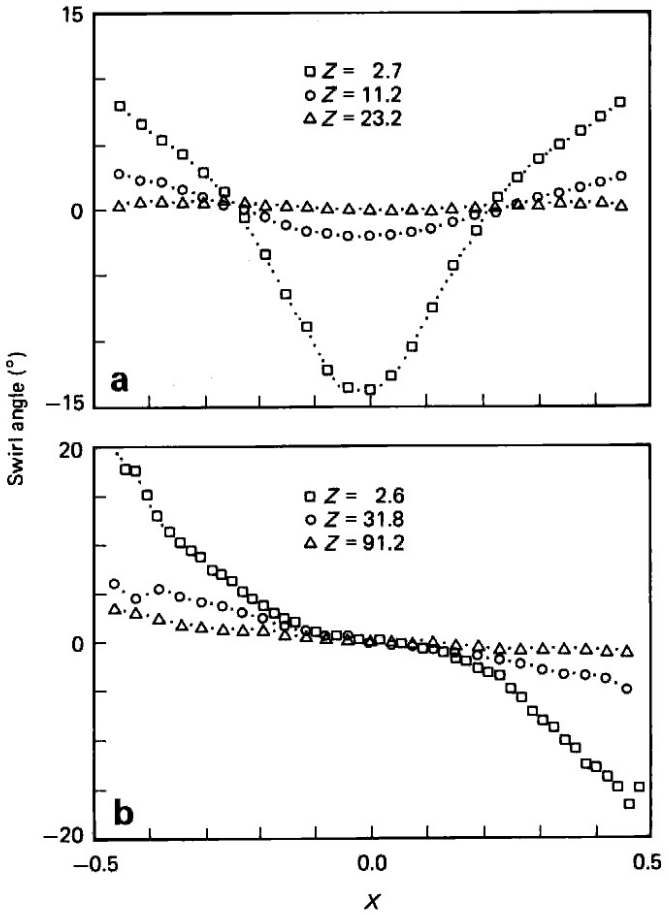

Figure 3 Swirl angle distributions produced by: (a) the single elbow configuration, and (b) the closely coupled double elbows out-of-plane configuration. Downstream distances are in diameters

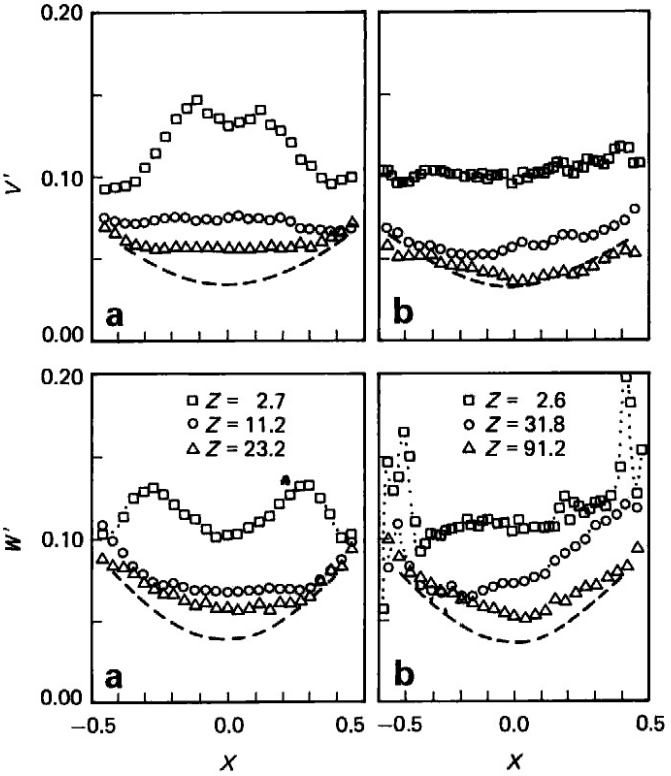

Figure 4 Cross-stream profiles of the root mean square values of the vertical, V', and streamwise, W', turbulent velocity components: (a) the single elbow, and (b) the closely coupled double elbows out-of-plane configuration. Downstream distances are in diameters. The dashed lines refer to Laufer's data

near the centre of the pipe while the flows near either pipe wall give angles of +8°.

The corresponding turbulent velocity distributions are presented in Figure 4(a). The dashed lines in these figures are the distributions measured by Laufer[9] in straight pipe in an airflow at Reynolds number 4×10^5. The turbulence measured in the present experiments is greater than that found by Laufer. However, Laufer's experimental arrangement had different inlet conditions, which are interpreted here as the explanation for the increased levels of turbulence found in the present experiments. These results show that the distributions of mean and turbulent velocities decay in different ways according to the type of swirl and the pertinent Reynolds number.

Double elbows out-of-plane

For this configuration where the two elbows are closely coupled, ($s = 0$ in Figure 1(b), i.e. no straight pipe separates them) intense, single-eddy (defined here as type I) swirl is created. Velocity profiles are shown in Figure 2(b) for Reynolds number 10^5. Details can be found in references 5 and 6.

Swirl angle distributions are presented in Figure 3(b) for a pipe Reynolds number of 10^5. These distributions show that in the downstream piping near these elbows: (1) swirl angles are about ±20° near the pipe walls and (2) in a core region about the centre of the pipe, the swirl angle is essentially zero, indicating that little or no swirl is present. This suggests that a flow conditioning element placed near the pipe wall could be very effective to reduce this swirl. This type of swirl is found to decay very slowly with downstream distance as compared to the single elbow swirl patterns described above.

The corresponding turbulent velocity distributions are presented in Figure 4(b). As noted above these distributions are different for those for the single elbow and from those measured by Laufer.

Decay of swirl

The decay of both types of swirl is shown in Figure 5 by the maximum swirl angles. These maximum swirl angle distributions are defined as half of the difference between the maximum and minimum swirl angles shown in Figure 3. In 20 diameters, the type II swirl has dissipated more than 90% (as quantified via the maximum value of the swirl angle) for a Reynolds number of 10^5. Single-eddy type swirl (type I) that is produced by two close-coupled elbows decays much more slowly. The swirl produced by spaced double elbows is much more complicated[6, 7]. It is a composite of type I and type II swirl depending on the length of the spacer, s. For a long spacer, the swirl should approach that of a single elbow case. The data for $s = 2.4D$ and $5.3D$ show that the type I swirl flow pattern still dominates the swirl interactions, although the initial swirl is much smaller than that for close-

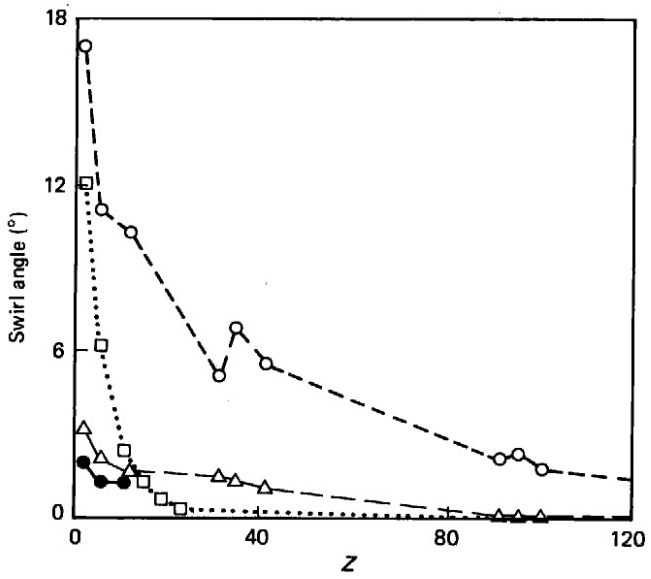

Figure 5 Streamwise distributions of the mean swirl angles for the single elbow configuration (□) and for the double elbows out-of-plane configurations (○ – closely coupled, △ – spaced at 2.4 diameters, and ● – spaced at 5.3 diameters)

coupled elbows. The decay of this swirl is also slow compared to that for type II swirl. The Reynolds number dependence of type I swirl shows that the decay rate decreases markedly as the Reynolds number increases[7]. Very long lengths of pipe are required to disspitate this single-eddy type swirl[8].

Other researchers[10–14] have described the decay of swirl as an exponential decay function of the following form:

$$S/S_0 = e^{-\alpha Z} \tag{1}$$

where S is some selected measure of the swirl (angular momentum, angular momentum flux, mean swirl angle, etc.), S_0 is the value of S where $Z = 0$, α is the swirl decay parameter, and Z is the number of diameters of straight, constant diameter piping downstream of the initial position where $S = S_0$. This function can be used for predicting the percentage of initial swirl as a function of the dimensionless axial distance Z.

The decay parameter, α, depends on the type of swirl, the selected measure of the swirl, and the pipe diametral Reynolds number, Re_D. To estimate the values of the various swirl decay parameters, a least squares fit of the experimental data was made for each swirl quantity, S, for each Reynolds number. This fit was produced using an iteration technique until the change in the squared error was less than 0.1%. If S is taken to be the maximum swirl angle, then at a Reynolds number of 10^5, α will be 0.026 and 0.186 for the single-eddy and double-eddy type swirls, respectively; at a Reynolds number of 10^4, α will be 0.029 and 0.201 for single-eddy and double-eddy type swirls, respectively. These equations show that swirl decays more slowly at higher Reynolds numbers. Therefore, the double-eddy swirl decays much faster than the single-eddy swirl at the same Reynolds number. Using these values we obtain the following Reynolds number dependencies. For the maximum swirl angle, we have:

for a single-eddy (type I) swirl

$$\alpha = 0.045\, Re_D^{-0.047} \tag{2}$$

for a double-eddy (type II) swirl

$$\alpha = 0.275\, Re_D^{-0.034} \tag{3}$$

These experimental results can also be used to evaluate the installation specifications in current flow measurement standards[1, 3]. For the case of a single elbow producing (type II) swirl angles of up to 19°, to reduce that swirl to less than 2° at a pipe Reynolds number of 10^5, about $12D$ would be required. The ISO-5167 specification of $36D$ for a 0.75 beta orifice meter for this situation would be very conservative, whereas the ANSI/API-2530 specification of 13.5 seems to be barely sufficient. For the case of a double elbow producing a single-eddy (type I) swirl of 20°, to reduce the swirl to less than 2° at a pipe Reynolds number of 10^5, about 89 diameters would be necessary. Neither ISO nor ANSI specifications would provide sufficient upstream length to reduce this swirl to the acceptable levels quoted. When Reynolds numbers are very high, i.e. 10^6 or 10^7, which can frequently occur in metering practice, the current specifications would appear to grossly underpredict the necessary upstream lengths for orifice meters installed downstream of this double elbow configuration.

While the decay analysis presented above is applied to the maximum value of the swirl angle found along the horizontal diameter, other swirl parameters can be generated as based upon angular momentum parameters and analysed to describe swirl decay phenomena. Several of these have been found to be very effective for accurately predicting the performance of different types of flowmeters when installation conditions are not ideal[5–8]. Because of differences in the mean and turbulent velocity distributions, the performance of some flowmeters installed in these pipeflows can be expected to be different from the performance expected in ideal pipeflow.

Pipe elbow effects on orifice meters

Orifice flowmeters of different geometries were calibrated in installations affected by the types of swirl described above. These were tested in a NIST 50 mm diameter water flow facility[5–8]. The orifice taps were the flange-type and oriented in the $X-Z$ plane and on the positive X-axis side, see Figures 1(a) and (b). The meter calibration results are considered in terms of shifts relative to the averaged discharge coefficient from ideal installation conditions. Ideal installation conditions would be where $200D$ of straight, constant diameter piping is installed upstream of the meter; about $25D$ of piping is installed downstream. The results were taken over the range of Reynolds numbers tested; these are, in terms of orifice hole to pipe diameter ratio (β): (1) $\beta = 0.363$, $15\,000 \leqslant Re_D \leqslant 45\,000$, (2) $\beta = 0.50$, $30\,000 \leqslant Re_D \leqslant 75\,000$, (3) $\beta = 0.75$, $45\,000 \leqslant Re_D \leqslant 100\,000$. It should be emphasized that, in the orifice effects described below, the discharge coefficients plotted for each position are mean values that are determined over the ranges of Reynolds numbers specified above. As such,

the values plotted have ranges associated with them and, therefore, definitive specifications can only be made within these tolerances. The Reynolds number ranges for the following results depend upon the beta ratio of the meter and specific values are given above. In this way, the results that follow should be taken in the appropriate context, that is, for the pertinent parameters of Reynolds number, beta ratio, relative pipe roughness etc.

Pipeflow effects on orifice geometries can be complex to interpret. It is apparent that velocity and swirl distributions together with turbulent profiles interact with fluid and flow conditions and the meter geometry to produce the observed discharge coefficients. The interpretations that follow focus on the flow phenomena that influence the pressure distributions in the regions of the pressure taps.

Figure 6(a) presents the effects of single elbow (type II) swirl on these meters; C_d is the orifice discharge coefficient. These results show that the single elbow flow reduces the discharge coefficients for these conditions. Relative to the ideal situation, these reductions range between −0.1% and −5.0%, when these meters are installed between 20 and 2.5D, respectively, from the elbow. The reduction of the discharge coefficient is largest for the installation nearest the elbow and the magnitude of the reduction increases with beta ratio.

Figure 6(b) presents the effects of the double elbows out-of-plane (type I) swirl on these meters. These results show that the double elbows out-of-plane flow can either increase or decrease discharge coefficients depending upon conditions. Increased discharge coefficients are speculated to be the result of type I swirl effects that reduce the orifice differential pressure. Decreased discharge coefficients can be explained by the flatness of the axial velocity distribution as compared to the ideal profile. This flatness would tend to increase the pressure at the upstream tap thereby increasing the pressure difference and thus reducing the discharge coefficient.

Increased discharge coefficients can be explained by swirl effects propagating through the orifice and elevating the pressure at the downstream tap via conservation of angular momentum principles. The relative significance of these effects is different for different beta ratios. It is shown elsewhere that these elbow flows influence orifice meters differently for different Reynolds number conditions[5–8, 13]. The erratic results found in Figure 6(b) for the largest beta ratio are interpreted to be the result of the complicated nature of this pipeflow very near the exit from this elbow configuration, see Figure 2(b).

Based on these orifice test results, it appears that the 2° limit on swirl angle is not a sufficient criterion to guarantee that orifice meter performance will be within ±0.5% of the ideal installation value. Specifically, for the 0.75 beta orifice meter the 2° swirl angle criterion indicates the meter should be installed 12D downstream of the single elbow configuration, but the shift in discharge coefficient at this location is found from Figure 6(a) to be −2%. Conversely, for the 0.363 beta orifice meter, the 2° swirl angle criterion is quite conservative since the discharge coefficient shift is only −0.25% at this location. If a ±0.5% tolerance on

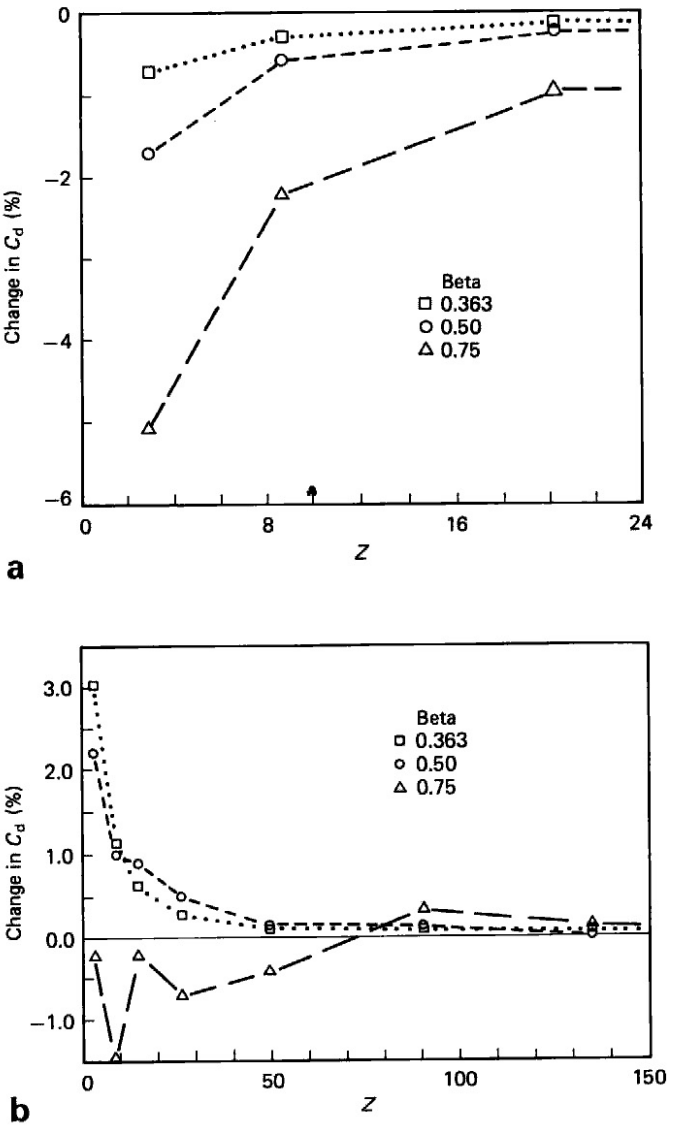

Figure 6 Calibration results for orifice-type meters installed in non-ideal conditions downstream of: (a) a single elbow; (b) a closely coupled double elbows out-of-plane configuration

the discharge coefficient is allowed for the 0.363 beta meter downstream of the single elbow, this can be achieved with $Z = 8$ (where the swirl angle is 4°). Furthermore, for the closely coupled double elbow configuration, the 2° swirl angle criterion produces discharge coefficient shifts less than ±0.5% for all beta ratios. For an installation criterion based upon ±0.5% shift in the discharge coefficient, our results show that: (1) a 0.75 beta orifice meter requires $Z = 50$ (where the swirl angle is greater than 4°), and (2) a 0.363 beta meter requires only $Z = 20$ (where the swirl angle is 8°).

Pipe elbow effects on turbine-type flowmeters

A specific type of turbine flowmeter was tested downstream of the single and closely coupled double elbows out-of-plane configurations. Results are shown in Figure 7, where the ordinate is the mean value of the change in the Strouhal number – relative to that in the ideal installation conditions over the flowrate

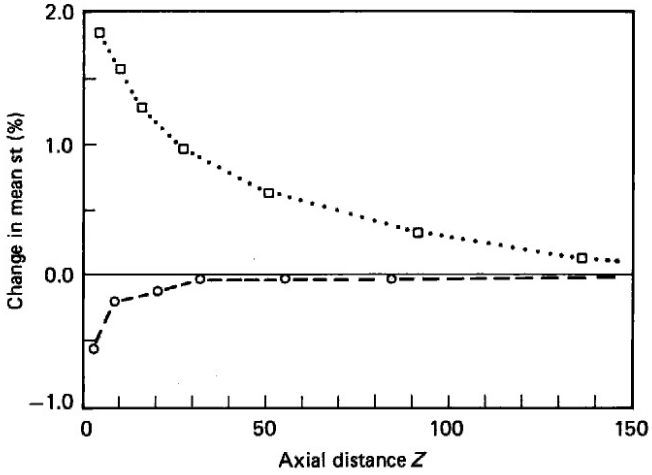

Figure 7 Calibration results for a turbine-type meter installed in non-ideal conditions downstream of single (○) and double elbows out-of-plane (□) configurations

range, $45\,000 \leq Re \leq 100\,000$. The Strouhal number is a dimensionless meter factor. This meter is designed so that the propeller rotates counter-clockwise looking downstream. Consequently, for installation positions near the double elbows out-of-plane configuration a positive shift occurs in meter factor. Therefore, in the flow field shown via Figures 2(b) and 3(b), the meter factor results in Figure 7 show shifts up to almost +2% depending upon meter position downstream from the exit plane of the double elbows out-of-plane configuration. Downstream from the single elbow the meter factor shifts downward to a lower limit of about −0.5%. This downward shift is interpreted to be due to a spatial averaging effect of the turbine propeller over the type II swirl and the altered distribution of axial velocity. It is also noted in Figure 7 that for downstream installation locations of $20-30D$, the meter factor shift is very small for the single elbow case, while for the double elbow situation the positive shift in meter factor is about 1%.

Although the discharge coefficient shifts described in the previous section and the meter factor shifts given above can be large and positive or negative, it is feasible to predict flowmeter performance in such non-ideal installation conditions[5–8]. Alternatively, the installation of flow conditioners downstream of pipework disturbances can be done to try to improve the pipeflow so that flowmeter performance is satisfactory.

Flow conditioners are designed using several strategies. Early designs attempted to remove swirl while adding only small increases to frictional pressure loss to that of the piping system. Other designs were intended to generate intense turbulent mixing which was to efficiently produce the ideal pipeflow distribution that would occur via very long lengths of straight, constant diameter piping. Still other designs attempted to produce the same pipeflow distribution regardless of the upstream piping configuration; these invariably had considerable pressure losses associated with them. Of all these types of flow conditioners, the tube bundle type is probably the most prevalently used and, for this reason, it was selected for testing in the current phase of this programme.

Tube bundle effects

For the tests described below, the tube bundle-type flow conditioner shown in Figure 8(a) was installed as shown in Figure 8(b). This tube bundle geometry was selected for the 50 mm diameter pipe to produce a geometrically scaled version of the shape that is conventionally used in US orifice metering practice. The small tubes are 9.5 mm in diameter, with wall thickness of 0.4 mm. For the Reynolds number ranges covered by the present tests, the results obtained should be identical to the many practical installations – in gases and liquids – where pertinent, non-dimensional parameters are duplicated.

Profile measurements are presented in Figure 9 for the vertical and streamwise components of the mean velocity both upstream and downstream of the tube bundle. Again, the dashed line shows the ideal distributions for these conditions. The profiles shown in Figures 9(a) and (b) that are measured at $Z = 2.6$ or 2.7 are distributions upstream of the tube bundle. In Figures 9(b), the profile labelled with an asterisk refers to a distribution measured with the tube bundle removed, that is, the same profile as shown in Figures 2(b). Since these distributions shown in Figures 2(a) and 9(a) were found to be the same, the profile between the tube bundle and the double elbow configuration was not remeasured but the asterisk is

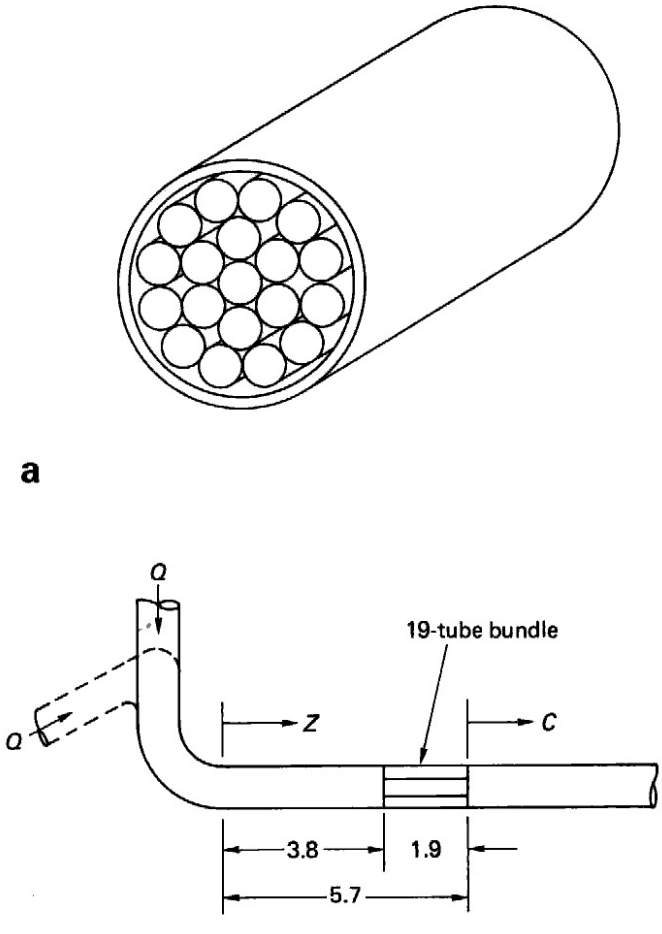

Figure 8 Flow conditioning arrangements: (a) tube bundle geometry; and (b) installation relative to elbow configurations

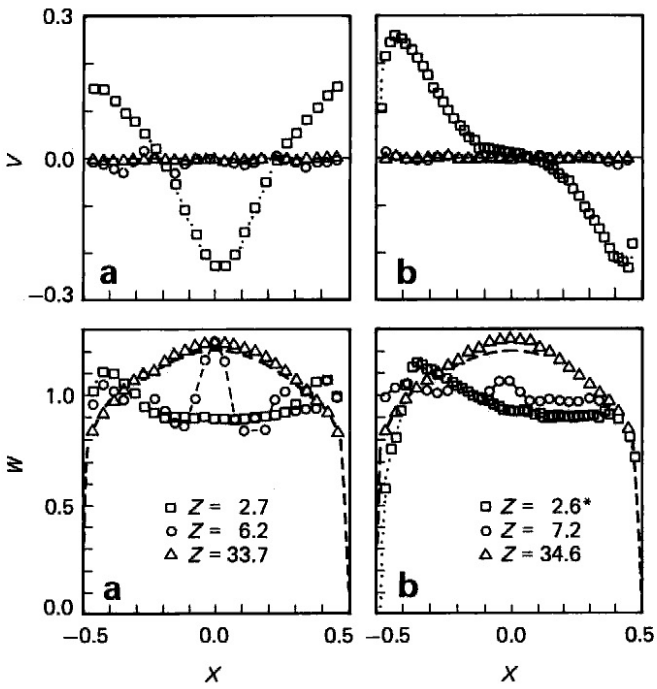

Figure 9 Vertical, V, and streamwise, W, velocity profiles upstream and downstream of the tube bundle installed downstream of: (a) the single elbow and (b) the double elbows out-of-plane configuration. Downstream distances are in diameters. Ideal profiles are shown by dashed lines

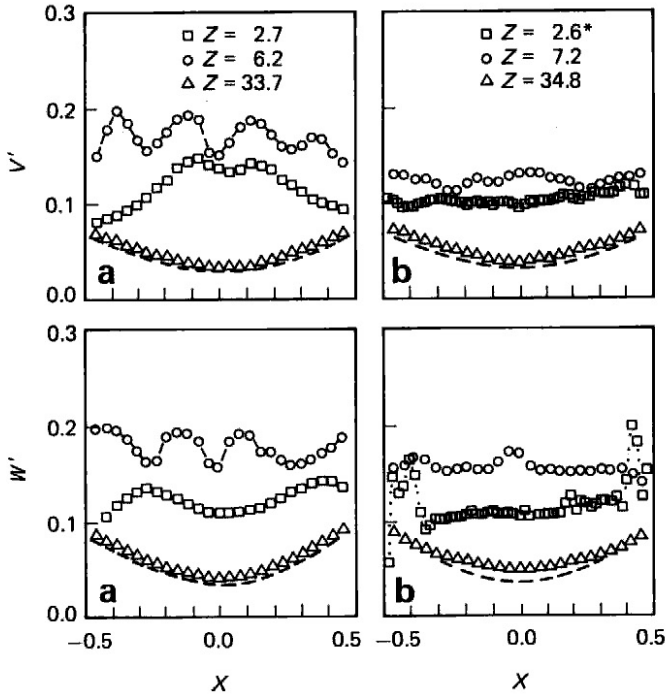

Figure 10 Cross-stream profiles of the root mean square values of the vertical, V', and streamwise, W', turbulent velocity components upstream and downstream of the tube bundle installed downstream of: (a) the single elbow and (b) the double elbows. Downstream distances are in diameters. The dashed lines refer to Laufer's data

inserted to denote the fact that these profiles are those shown in Figures 2(a). The profiles in Figure 9 that are measured downstream of the tube bundle clearly show both the swirl reduction and the jetting effects from the individual tubes. The vertical velocity distributions downstream of both elbow configurations and the tube bundle are essentially zero for all of the stations measured – thus showing how these conditioners successfully remove swirl. The streamwise velocity distributions just downstream of the tube bundle show, for the single elbow case, peaked values which align with the five tubes arranged essentially along the diameter of this tube geometry, see Figure 9(a). This effect is less conspicuous in the results for the double elbow configuration where the data is taken further downstream than that for the single elbow. At the most downstream station measured, the streamwise velocity distributions for both configurations are found to have flow in the central core of the pipe with velocities exceeding those for the ideal profiles. It appears that, for both of these piping configurations, the tube bundle produces flow effects that 'overdevelop' the pipeflow.

Figures 10(a) and (b) present results for the vertical and streamwise components of the turbulent velocity both upstream and downstream of the tube bundle for the single elbow and the double elbow configurations, respectively. The asterisk is noted in Figure 10(b) where it has the same meaning as described above for Figures 9(b). The results in Figures 10(a) show clearly, in the profile just downstream of the tube bundles, the effects of the peaked turbulence levels in the regions between the jetting effects noted in Figures 9(a). These effects are interpreted to be the results of the mixing processes which occur between the adjacent jetting flows from the individual tubes. These effects are less apparent in Figures 10(b) for the double elbow case where results are presented at a location further downstream. Figures 10(a) and (b) show that the profiles just downstream of the tube bundle have higher averaged levels of turbulence as compared to the cases without the tube bundle, see Figure 4. These enhanced turbulence distributions produced by the tube bundle may be influential in overdeveloping the pipeflows so that the streamwise profiles have the high speed core flows some $30D$ downstream from the exit plane of the elbow.

Tube bundle effects on orifice meters

For conditions duplicating those described above for the three orifice geometries, the calibrations were repeated downstream of the tube bundle. Figure 11(a) presents the effects on these meters of the single elbow followed by the tube bundle installed as shown in Figure 8(b). The abscissa, C, is the orifice location downstream from the tube bundle expressed in D, see Figure 8(b). The ordinate is the percentage change in the mean value of the discharge coefficient relative to that for the ideal installation as plotted in Figures 6(a) and (b). It is apparent that when these orifice meters are installed within $10D$ downstream from the tube bundle, the discharge coefficients are lowered in comparison with the values for the ideal installation. These reductions are dependent upon beta ratio. These results show that the discharge coefficient is markedly

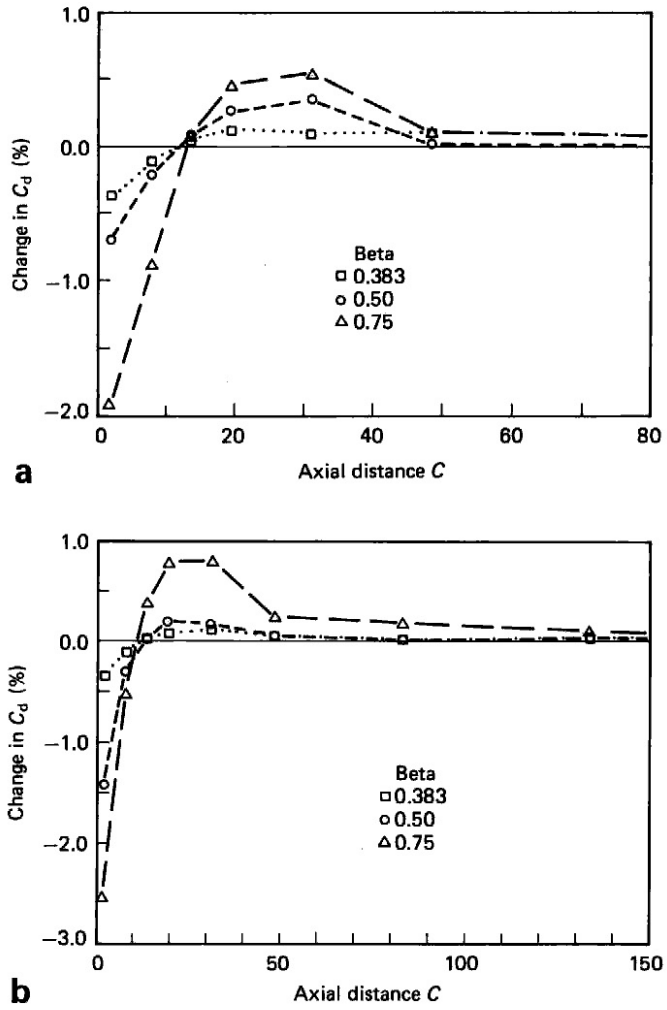

Figure 11 Calibration results for orifice-type meters installed downstream of: (a) a single elbow and a tube bundle flow conditioner, and (b) a closely coupled double elbows out-of-plane configuration and a tube bundle flow conditioner

reduced when the meter is installed within 11 to 13D from the exit plane of the tube bundle. From the streamwise velocity profiles measured in these pipe intervals, it is found that these profiles are relatively uniform and are undoubtedly influential in producing these reduced changes in discharge coefficients. This profile uniformity is concluded to elevate the pressure levels in the flow near the upstream pressure tap location over that level which would prevail for the ideal orifice installation. This effect increases the pressure difference across the meter thereby lowering the discharge coefficient. The magnitude of these effects increases with the beta ratio as shown in Figure 11(a).

The orifice discharge coefficient distribution for installation positions further downstream than the 11 to 13D location show positive shifts relative to those for ideal conditions. Such results can be interpreted as being due to the overdeveloped distributions measured for the streamwise component of the time-averaged profiles shown in Figure 9(a). For these profiles the pressure levels in the region near the upstream taps are lowered because the flow velocity near the pipe wall is lower than that for the ideal conditions, thereby reducing the differential pressure across the meter and thus increasing the discharge coefficients. These positive shifts in orifice discharge coefficients persist for these conditions, to about the 50D location. It is expected that, for different Reynolds number or roughness conditions, the levels of coefficient shifts as well as the orifice location intervals will vary.

Figure 11(b) presents orifice discharge coefficient results for installations downstream of the double elbows out-of-plane and the tube bundle. Again, orifice effects similar to those observed for the single elbow and tube bundle are found. For orifice installation positions closer than about 12 to 15D to the exit plane of the tube bundle, discharge coefficient shifts are negative. The explanation given is the same as that given above for the negative shift found for the single elbow. For corresponding locations and beta ratios, the negative shifts found for the double elbows out of plane and tube bundle configuration are larger in magnitude than those for the single elbow and tube bundle. When these orifice meters are located further downstream than the 12 to 15D position, the discharge coefficient shifts are positive. Again, explanations are the same as given above. It is also noted that the levels of coefficient shifts are equal to or greater than those for the single elbow and tube bundle arrangement. For the largest beta ratio, the positive shifts in orifice discharge coefficient persist with orifice installation position, C, and can be detected until or beyond the 100D location.

It is concluded that the effects of tube bundle flow conditioners significantly alter pipeflows. Although some quantitative differences are observed in coefficient shifts these alterations are shown to produce the same generic quantitative patterns on the performance of orifice meters installed downstream. Therefore, it appears that tube bundle effects on orifice meters appear to be the main source of the disturbed orifice performance and upstream piping configurations appear to be less significant.

Tube bundle effects on a turbine-type meter

For conditions duplicating those described above, the calibrations were repeated for the turbine-type flowmeter downstream of the tube bundle. Figure 12 presents these effects versus the axial distance, C, defined as before. These results show that this flow conditioner reduces the Strouhal number shift for installations downstream of the double elbows out-of-plane to less than about +0.2%. These results can be interpreted as due to the fluid interactions with the meter geometry – its design and bearing characteristics and the pertinent fluid and flow parameters. While the vertical velocity distribution presented in Figure 9(b) shows that the tube bundle has essentially removed the swirl from the pipeflow, both the mean axial velocity distribution and the turbulence profiles shown in Figure 10(b) are not the equilibrated profiles. In spite of this, this meter shows performance characteristics close to 'ideal' when this tube bundle is used and the meter is installed 10D or more downstream from it.

The Strouhal number results downstream of the single elbow and tube bundle indicate reduced shifts for $C \leqslant 15$. However, for meter installations closer than 10D from the tube bundle, this meter exhibits

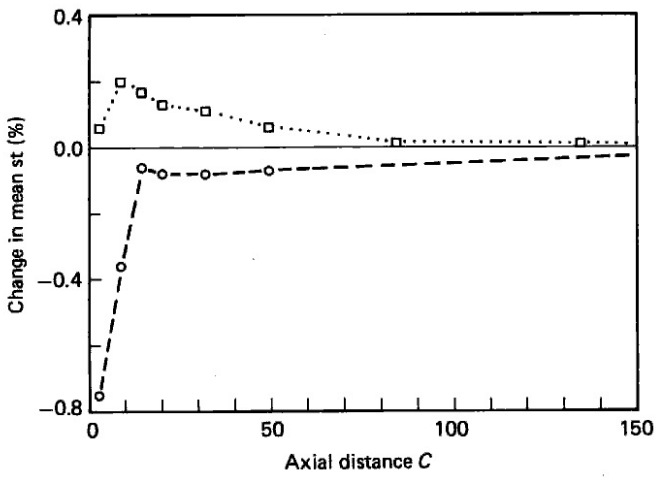

Figure 12 Calibration results for a turbine-type meter installed downstream of single (○) and double elbows out-of-plane (□) configurations and tube bundle flow conditioner

shifts which equal or exceed those for corresponding distances from the elbow without the tube bundle. For example, if this meter should be installed $10D$ from the single elbow, Figure 7 shows that a mean meter factor shift of about −0.2% can be expected. If a tube bundle is installed between the elbow and meter as shown in Figure 8, then since $Z = C + 5.7$, this situation corresponds to about $C = 4$. Figure 12 shows that for $C = 4$, the mean meter factor shift is about −0.75%. Therefore, it appears that it is important to understand how specific meters respond to specific, non-ideal, meter installation effects before tube bundle flow conditioners are indiscriminantly used.

Discussion

To improve the performance of the types of meters described above, a number of conventional strategies can be used. Firstly, a prevalent strategy has been to perform a calibration using the identical conditions of fluid, piping, meter, flowrate range etc. However, this is not always feasible or convenient.

Secondly, the use of flow conditioning elements installed in the piping between the elbow configuration and the meter can possibly produce improved metering performance. These flow conditioning elements vary widely in their geometrical arrangements; their conditioning capabilities can be dependent on the type of pipeflow and their geometry; they can cause significant pressure losses in the pipeflow[15]. In view of the present results, flow conditioner and flowmeter combinations should be tested together. The present results also indicate that the widely used tube bundle which does remove swirl can also produce some significant negative or positive shifts in meter performance depending upon conditions.

Thirdly, it has recently been demonstrated that satisfactory metering performance can be successfully predicted and achieved without resorting to flow conditioners if sufficient data is available on the non-ideal pipeflow and data is obtained for how the respective meter is shifted with respect to the non-ideal pipeflow.[5–7] By correlating the pipeflow data with the meter shifts, it has been demonstrated that it is feasible to adjust the ideal meter performance so that accurate flow measurements can be obtained in the non-ideal meter installations[8, 16].

Although not investigated here, the role of pipe roughness on swirl decay has been studied elsewhere. Mottram and Rawat[17] have shown that increased pipe roughness can reduce the lengths of piping required to dissipate pipeflow swirl.

Conclusions

Different piping configurations produce different types of swirl patterns. The decay of swirl is dependent on the Reynolds number and the type of swirl. Installation specifications in the current flow measurement standards are concluded to be insufficient. This is especially true if strong, single-eddy (type I) swirl is present. In this case, extremely long lengths of pipe are required to naturally dissipate this type of swirl at high Reynolds numbers. Meter installations where measurement accuracy is important should be re-evaluated to ensure that disturbed pipeflow phenomena do not detrimentally affect the particular meter in the specific location.

It is concluded that the 2° swirl angle criteria for orifice installations should be re-evaluated. All significant factors that can influence orifice performance should be incorporated into such specifications.

The effects of single and double eddy types of swirl are found to significantly change the performance of orifice and turbine type flowmeters. These shifts in performance vary both in direction and in magnitude depending on the type and strength of swirl, Reynolds number and the specific type and design of the flowmeter.

The effects of tube bundle-type flow conditioners are found to effectively reduce swirl. However, it is also found that tube bundle effects radically alter orifice meter performance. These effects cause negative shifts in orifice discharge coefficients relative to ideal values for all three of the beta ratios tested when these meters are installed near the tube bundle. When the meter is installed further downstream from the tube bundle, the shift is reduced to zero but then becomes positive when positions further downstream are tested. These positive shifts are interpreted to be due to the overdeveloped, streamwise velocity profiles observed for both piping configurations in these locations. When very distant meter locations are tested, the positive shift reduces asymptotically to zero.

To the suggestion that orifice installations be specified according to the position downstream of the tube bundle where this shift changes sign, our conclusion would be that this solution may not give satisfactory results for all conditions due to a number of reasons. Firstly, the sensitivity of orifice discharge coefficient to downstream orifice position is significant for specific conditions such as larger beta ratios. Therefore, if small deviations in actual installation locations were to occur, the discharge coefficient could be changed significantly. Additionally, this orifice location where the discharge coefficient changes sign could be dependent upon a number of other factors such as Reynolds number range, relative pipe

roughness etc. Consequently, it is concluded that a satisfactory specification for an orifice meter downstream of this type of tube bundle could be quite complicated – especially when the practical ranges of Reynolds number and relative roughness can vary so widely.

The conclusions for the turbine meter test results indicate that while tube bundle flow conditioners can remove swirl from pipeflows, this should not imply that ideal meter performance can be expected. On the contrary, the single elbow results show that for a specific meter installation some $10D$ from the single elbow configuration, a mean meter factor shift of some -0.2% occurred. The remedial insertion of a conventional tube bundle caused this shift to increase to about -0.8%. Therefore, the important conclusion here is that meter performance should be based upon pertinent test results or a fundamental understanding of the flow effects not only produced by flow conditioning elements but also affecting flowmeters, or both.

Acknowledgements

This research is supported by an industry–government consortium formed by NIST to conduct critical research on generic fluid measurement topics. The members of this consortium as of June 1990 are: Ketema–McCrometer, Chevron Oil, Controlotron, Dow Chemical, E. I. DuPont de Nemours, Ford Motor Co., Gas Research Institute, Gas Unie, ITT Barton, Kimmon Mfg. Ltd., Equimeter and Rosemount. Special acknowledgement is given to Dr K. M. Kothari of the Gas Research Institute for his technical input and support for this programme. The technical efforts put forth by Mr B. L. Shomaker in producing the experimental piping configurations and assisting with other technical matters are gratefully acknowledged. Last, but certainly not least, the competent secretarial capabilities of Mrs G. M. Kline are gratefully acknowledged for her patient preparations of numerous drafts of this paper.

References

1 Orifice metering of natural gas and other related hydrocarbon fluids. AGA Report No. 3, Second Edition (1985) American Gas Association, Arlington, Virginia. This document is alternatively named ANSI/API-2530

2 **Mattingly, G. E., Spencer, E. A. and Klein, M.** Workshop on fundamental research issues in orifice metering, Gas Research Inst. (GRI) Rept. 84/0190, (Sept. 1984)

3 Measurement of fluid flow by means of orifice plates, nozzles and venturi tubes inserted in circular cross-section conduits running full. International Organization for Standardization, ISO 5167-1980(E), First edition

4 **Yeh, T. T., Robertson, B. and Mattar, W. D.** LDV measurement near a vortex shedding strut mounted in a pipe. *ASME J. Fluid Engng.* **105** (June 1983) 185–196

5 **Mattingly, G. E. and Yeh, T. T.** Flowmeter installation effects. Proc. Annual NCSL Symp., Washington, DC (August 1988)

6 **Mattingly, G. E. and Yeh, T. T.** NBS industry–government consortium research program on flowmeter installation effects: Summary report with emphasis on research period July–December 1987. NISTIR 88–3898 (November 1988)

7 **Mattingly, G. E. and Yeh, T. T.** NBS industry–government consortium research program on flowmeter installation effects: Summary report with emphasis on research period January–July 1988. NISTIR 89–4080 (April 1989)

8 **Yeh, T. T. and Mattingly, G. E.** Prediction of flowmeter installation effects. Presented at the American Institute of Chemical Engineers 1989 Spring National Meeting, Houston, Texas, April 2–6, 1989, Paper 51e

9 **Laufer, J.** The structure of turbulence in fully developed pipe flow. NBS Rept. 1974 (Sept. 1952)

10 **Fejer, A., Lavan, Z. and Wolf, Jr, L.** Study of swirling fluid flow. ARL68-0713, Aerospace Research Laboratories, USAF, Wright-Patterson Air Force Base, Ohio (October 1968)

11 **Kreith, F. and Sonju, O. K.** The decay of a turbulent swirl in a pipe. *J. Fluid Mech.* **22**(2) (1965) 257–271

12 **Miller, R. W.** Flow measurement engineering handbook. McGraw-Hill, New York, NY (1983)

13 **Norman, R., et al.** Swirl decay in pipeflow. Proc. 1989 International Gas Research Conf., Tokyo

14 **Musolf, A. O.** An experimental investigation of the decay of turbulent swirl flow in a pipe. MS Thesis, University of Colorado, Department of Civil Engineering (1963)

15 **Miller, R. W.** Flow measurement engineering handbook, McGraw-Hill, New York (1985)

16 ASME MRC-10M-1988, Method for establishing installation effects on flowmeters. Amer. Soc. Meçh. Engrs (ASME), New York, NY

17 **Mottram, R. C. and Rawat, M. S.** Attenuation effects of pipe roughness on swirl and the implications for flowmeter installation. Int. Symp. Fluid Flow Meas. Amer. Gas Assoc., Arlington, VA (1986)